MCB
Journals.ASM.org

Serine Phosphorylation Sites on IRS2 Activated by Angiotensin II and Protein Kinase C To Induce Selective Insulin Resistance in Endothelial Cells

Kyoungmin Park,[a] Qian Li,[a] Christian Rask-Madsen,[a] Akira Mima,[a] Koji Mizutani,[a] Jonathon Winnay,[a] Yasutaka Maeda,[a] Katharine D'Aquino,[b] Morris F. White,[b] Edward P. Feener,[a] George L. King[a]

Section of Vascular Cell Biology, Joslin Diabetes Center, Harvard Medical School, Boston, Massachusetts, USA[a]; Children's Hospital Boston, Boston, Massachusetts, USA[b]

Protein kinase C (PKC) activation, induced by hyperglycemia and angiotensin II (AngII), inhibited insulin-induced phosphorylation of Akt/endothelial nitric oxide (eNOS) by decreasing tyrosine phosphorylation of IRS2 (p-Tyr-IRS2) in endothelial cells. PKC activation by phorbol ester (phorbol myristate acetate [PMA]) reduced insulin-induced p-Tyr-IRS2 by 46% ± 13% and, similarly, phosphorylation of Akt/eNOS. Site-specific mutational analysis showed that PMA increased serine phosphorylation at three sites on IRS2 (positions 303, 343, and 675), which affected insulin-induced tyrosine phosphorylation of IRS2 at positions 653, 671, and 911 (p-Tyr-IRS2) and p-Akt/eNOS. Specific PKCβ2 activation decreased p-Tyr-IRS2 and increased the phosphorylation of two serines (Ser303 and Ser675) on IRS2 that were confirmed in cells overexpressing single point mutants of IRS2 (S303A or S675A) containing a PKCβ2-dominant negative or selective PKCβ inhibitor. AngII induced phosphorylation only on Ser303 of IRS2 and inhibited insulin-induced p-Tyr911 of IRS2 and p-Akt/eNOS, which were blocked by an antagonist of AngII receptor I, losartan, or overexpression of single mutant S303A of IRS2. Increases in p-Ser303 and p-Ser675 and decreases in p-Tyr911 of IRS2 were observed in vessels of insulin-resistant Zucker fatty rats versus lean rats. Thus, AngII or PKCβ activation can phosphorylate Ser303 and Ser675 in IRS2 to inhibit insulin-induced p-Tyr911 and its anti-atherogenic actions (p-Akt/eNOS) in endothelial cells.

Insulin resistance is one of the major risk factors for developing atherosclerosis, unsuppressed hepatic gluconeogenesis, and impaired glucose uptake into muscle and adipose tissue (1, 2). Recently, substantial evidence has been obtained that insulin has important effects on the vascular endothelium via the activation of IRS/p85/PI3K (phosphatidylinositol 3-kinase)/Akt, with increases in endothelial nitric oxide (eNOS), heme oxygenase 1 (HO-1), and vascular endothelial growth factor (VEGF) expression (3). In insulin-resistant states, the selective loss of insulin action on the vascular endothelium via the loss of insulin activation of IRS/p-Akt can cause endothelial dysfunction, which correlates with the increased risk of coronary artery disease and accelerated development of atherosclerosis (4). We have reported that endothelial insulin receptor apoE knockout mice (EIRAKO) with double knockout of apolipoprotein E ($apoE^{-/-}$) and insulin receptor ($IR^{-/-}$) developed significantly more atherosclerosis than $apoE^{-/-}$ mice, suggesting the physiological importance of insulin for endothelial cells (4). Recent studies have shown clearly that multiple factors can selectively inhibit insulin action via the activation of IRS/PI3 kinase and Akt pathways, such as hyperglycemia, free fatty acids, protein kinase C (PKC) activation, angiotensin, and diabetes (5–8). Although both IRS1 and IRS2 are expressed on the endothelium, it remains unclear whether they can induce similar profiles of action, since both can activate PI3 kinase and p-Akt. Under pathophysiological conditions such as insulin resistance and obesity, one of the possible mechanisms for selective endothelial insulin resistance is accelerated proteasomal degradation of IRS2 (9, 10).

IRS proteins are regulated through multiple reversible post-translational modifications, most importantly by phosphorylation (11, 12). The amino acid sequences of IRS1 and IRS2 provide a multitude of tyrosine, serine, and threonine residues as potential phosphorylation sites. Multiple sites for tyrosine phosphorylation (p-Tyr) of both IRS1 and IRS2 isoforms have been identified and analyzed, and they are needed for the transduction of insulin's metabolic signaling (12). In addition to the tyrosine sites, the function of serine/threonine phosphorylation (p-Ser/Thr) is on sites known to negatively regulate insulin signaling (13, 14). Approximately 124 potential p-Ser/Thr sites for IRS1 have been identified, and more than 30% of these sites have been studied in detail. Many of these sites have seen shown to affect insulin activation (15–18). For IRS2, a similar number, 129, of potential and verified p-Ser/p-Thr sites have been identified, but very few of these sites have been studied, and their vascular effects are completely unknown (12, 19).

Activation of PKC isoforms, especially the β and δ isoforms, has been reported to inhibit insulin action in the endothelium in response to diabetes or insulin resistance to cause endothelial dysfunction (20–23). Furthermore, inhibition of PKCβ isoforms by an isoform-selective antagonist improved insulin sensitivity in the endothelium and decreased severity of atherosclerosis in $apoE^{-/-}$ mice (22, 24). Recently, we reported that PKC activation by phorbol esters (PMA) and AngII selectively inhibited insulin-induced phosphorylation of PI3K/eNOS and caused endothelial dysfunc-

Received 26 April 2013 Returned for modification 10 May 2013
Accepted 6 June 2013
Published ahead of print 17 June 2013
Address correspondence to George L. King, George.king@joslin.harvard.edu.
K.P. and Q.L. contributed equally to this work.

doi:10.1128/MCB.00506-13

tion by decreasing p-Tyr-IRS2 but, surprisingly, not IRS1 in aortic endothelial cells (7).

In this study, we identified the serine phosphorylation (p-Ser) sites induced by PKC activation or AngII, which inhibits insulin-induced p-Tyr sites on IRS2 and its signals in endothelial cells. We have corroborated the presence of these p-Tyr/Ser sites on IRS2 by comparative analysis of their levels in microvessels from lean and insulin-resistant fatty rodents. These studies provide information on the changes in p-Ser of IRS2 of the insulin signaling cascade causing selective endothelial dysfunction.

MATERIALS AND METHODS

Chemicals and antibodies. Ruboxistaurin (RBX) was purchased from Millipore (Billerica, MA). Losartan potassium (losartan) and *S*-(+)-PD 123177 trifluoroacetate salt hydrate (PD123177) were purchased from Sigma (St. Louis, MO). Antibodies to Flag and histidine and specific antibody for p-Tyr911 were purchased from Sigma (St. Louis, MO). The rabbit polyclonal antibodies for p-Tyr, p-Ser270, and p-Ser307 of IRS1 were purchased from Santa Cruz Biotechnology, Inc. (Santa Cruz, CA). The rabbit polyclonal antibodies for phosphorylated and total Akt and Erk were purchased from Cell Signaling Technology (Danvers, MA). Goat polyclonal antibody against β-actin was purchased from Santa Cruz Biotechnology, Inc. (Santa Cruz, CA). Rabbit polyclonal antibody against p-Tyr was purchased from Santa Cruz Biotechnology (Santa Cruz, CA). Polyclonal antibody against insulin receptor β (IRβ) was purchased from Santa Cruz Biotechnology (Santa Cruz, CA), and monoclonal antibody for p-Ser636/639 of IRS1 was purchased from Cell Signaling Technology (Danvers, MA). Antibodies against IRS1, IRS2, and p-Ser632 of IRS1 were purchased from Santa Cruz Biotechnology, Inc. (Santa Cruz, CA), and Millipore (Billerica, MA).

Cell culture. Bovine aortic endothelial cells (BAEC) were cultured in Dulbecco's modified Eagle's medium (DMEM; provided by Joslin Media Core) supplemented with 10% fetal bovine serum and antibiotics and grown on culture dishes precoated with 0.2% gelatin (Sigma, St. Louis, MO). The cells were used at less than passage 5. Mouse lung endothelial cells (LEC) were cultured in DMEM supplemented with 10% fetal bovine serum (FBS), 100 mg/liter of heparin, and 50 mg/liter of endothelial cell growth supplement (ECGS). The procedure for isolation of lung endothelial cells from mice was previously described (7).

Transfection and transduction. For transient transfection, BAEC were transfected with plasmids using Lipofectamine 2000 (Invitrogen, Carlsbad, CA) according to the manufacturer's protocol. For infection with adenovirus expressing a constitutively activated wild form of PKC (α, β1, β2, δ, or ε) and dominant negative form of PKCβ2 (Ad-DN-PKCβ2), BAEC in 6-well plates were seeded in growth medium and cultured for 24 h. The cells were infected with Ad-IRS1, Ad-IRS2, Ad-PKCα, -β1, -β2, -δ, or -ε, Ad-DN-PKCβ2, or Ad-GFP virus at a multiplicity of infection (MOI) of 5, as previously described.

Animals. All of the animal experiments were performed in compliance with the Joslin Diabetes Center Statement for the Use of Animals in Diabetic Research. Male obese Zucker rats (*fa/fa*) and their age-matched lean controls (*fa/+*) were purchased from Charles River Laboratories (Wilmington, MA). The rats (12 weeks old) were fed standard rodent chow and water. Physiological parameters of the Zucker obese and lean rats were measured before experiments were performed. Rats were sacrificed with CO_2, and the aorta and epididymal fat pads were isolated immediately. The aortas were kept in DMEM containing 0.1% bovine serum albumin (BSA) at room temperature for 2 h before insulin stimulation and then were frozen with liquid N2 and kept at −80°C for subsequent analysis.

Western blotting, cellular fractionation, and immunoprecipitation (IP). BAEC and mouse lung endothelial cells were synchronized with 0.1% BSA (Sigma, St. Louis, MO) overnight, pretreated with 100 nM PMA for 20 min, and stimulated with 100 nM insulin for 10 min. Cells were washed with cold PBS and lysed in radioimmunoprecipitation assay (RIPA) buffer (150 mM NaCl, 1% NP-40, 0.1% SDS, 50 mM Tris-HCl [pH 8.0], 1 mM EDTA, and 1 mM phenylmethylsulfonyl fluoride [PMSF]). For *in vivo* assays, the aortic tissues were frozen in dry ice and homogenized in 300 μl of ice-cold tissue lysis buffer (50 mM Tris-HCl [pH 7.8], 5 mM EDTA, 0.1% SDS, 1% NP-40, 2.5% glycerol, 100 mM NaCl, and 1 mM fresh PMSF). The lysates were cleared by centrifugation at 10,000 × *g* for 20 min at 4°C, and the protein concentration of the lysates was determined using the Bradford assay. Proteins were subjected to IP analysis.

For cellular fractionation, the membrane fraction was isolated using a fractionation system kit (Biovision, Mountain View, CA), and membrane protein concentration was measured using the Bradford assay. Equal amounts of membrane proteins were blotted with a mouse antibody for pan-cadherin (Santa Cruz Biotechnology, Inc., Santa Cruz, CA). For IP, the cells were lysed in the IP buffer (150 mM NaCl, 2 mM EDTA, 1% NP-40, 50 mM Tri-HCl [pH 7.4], 0.1% SDS, and 1 mM PMSF). Cellular or tissue lysates were incubated with the appropriate antibodies at 4°C overnight, followed by the addition of protein A/G Sepharose beads (Santa Cruz Biotechnology, Inc., Santa Cruz, CA) for 2 h at 4°C. The beads were then washed with washing buffer containing 150 mM NaCl, 1 mM EDTA, 1% NP-40, 10 mM Tris-HCl [pH 7.4], and 1 mM PMSF, and the precipitated proteins were subjected to SDS-PAGE followed by immunoblotting with the appropriate antibodies. The signal intensity was quantified using image J software (SynGene, Frederick, MD).

Serial p85α mutant purification. The expression vectors of the serial mutants of p85α tagged with a histidine sequence were provided by one of us (J.W.). All p85α mutants were expressed in *Escherichia coli* (SoluBL21) purchased from Genlantis Inc. (San Diego, CA) by IPTG induction. The recombinant proteins were purified by passing the supernatant of *E. coli* lysates through a Ni-resin column (Thermo Scientific, Rockford, IL).

Mass spectrometry. IRS2 was immunoprecipitated from cell lysates obtained from PMA-stimulated BAEC, separated by SDS-PAGE, and stained with Coomassie brilliant blue G-250 stain. Gel slices containing IRS2 were digested with 5 ng/μl sequencing grade-modified trypsin (Promega) in 25 mM ammonium bicarbonate containing 0.01% *n*-octylglucoside for 18 h at 37°C. Peptides were eluted from the gel slices with 80% acetonitrile, 1% formic acid. Tryptic digests were separated by capillary high-performance liquid chromatography (HPLC; C_{18} Picofrit column, 75-μm inside diameter; New Objective) using a flow rate of 100 nl/min over a 3-h reverse phase gradient and analyzed using an linear trap quadrupole (LTQ) 2-dimensional linear ion trap mass spectrometer (ThermoFisher). Resultant tandem mass spectrometry (MS/MS) spectra were matched against IRS2 sequence using Mascot (Matrix Science) and TurboSequest (BioWorks 3.1) with a fragment ion tolerance of <0.5 and amino acid modification variables, including phosphorylation (80 Da) of Ser, Thr, and Tyr and oxidation (16 Da) of Met.

Statistical analysis. Data are presented as means and standard errors of the means (SEM). Comparisons between groups were performed with unpaired Student's *t* test. Multiple comparisons were performed with one-way analysis of variance, and the Student-Newman-Keuls method was used for *post hoc* tests. *P* values less than 5% were considered statistically significant.

RESULTS

Effect of PKC activation on insulin-induced tyrosine phosphorylation on IRS2. Insulin (100 nM) increased p-Tyr-IRS2 in BAEC infected with Ad-IRS2 as shown in Fig. 1A and B. Increasing the expression of IRS2 significantly enhanced the actions of insulin on p-Tyr-IRS2 and p-Akt by 2.2- and 3.5-fold, respectively. Activation of PKC by PMA (100 nM), a diacylglycerol (DAG) analog and general PKC activator, significantly inhibited insulin-induced p-Tyr of IRS2 by 46% ± 15% and p-Akt by 57% ± 11% in BAEC (Fig. 1A, B, and C). Similarly, PMA has an inhibitory effect on insulin-induced tyrosine phosphorylation of endogenous IRS2 (Fig. 1D). Consistent

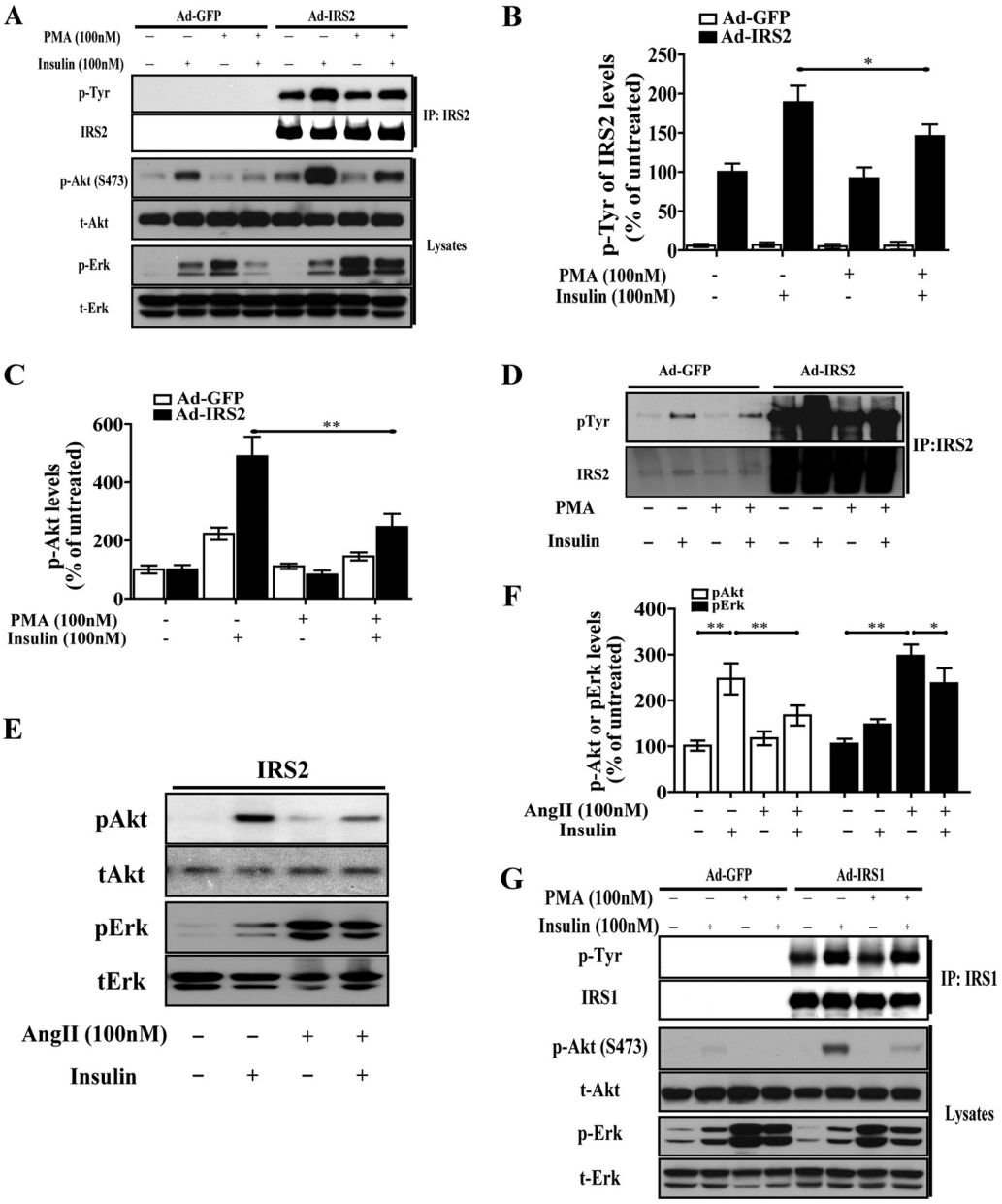

FIG 1 PMA and AngII inhibit insulin-induced p-Tyr in the IRS2 and PI3K pathway in BAEC. (A) Inhibitory effect of PMA on insulin-induced signaling. Cells were incubated with PMA (100 nM) for 20 min. Insulin (10 nM) was added after PMA treatment for 10 min. Immunoblot analysis of tyrosine phosphorylation was carried out after IP by anti-IRS2 antibody in the BAEC, overexpressing IRS2 after treatment with insulin, PMA, and PMA plus insulin. (B) Quantification of p-Tyr levels in IRS2. (C) p-Akt levels in the total cell lysates of BAEC treated as described for panel A. (D) PMA inhibited insulin-induced p-Tyr level in endogenous IRS2. (E) Immunoblot analysis of p-Akt and p-Erk in lysates from BAEC expressing WT-IRS2 treated with insulin in either the absence or presence of AngII. (F) p-Akt and p-Erk were quantified by densitometry, and levels are expressed as percentages of that in untreated cells (means ± SEM, $n = 3$). (G) Inhibitory effect of PMA on insulin-induced signaling in overexpression of IRS1.

with the inhibitory effect of PMA on p-Akt, AngII also inhibited insulin-induced p-Akt by 28% ± 11% in BAEC (Fig. 1E and F). Induction of p-Erk by insulin, however, was very different from that of p-Akt, since PMA alone increased basal p-Erk by 225% ± 31%, which was not enhanced by the overexpression of IRS2. In combination with insulin, induction of p-Erk by PMA or AngII was decreased by 42% ± 22% and 15% ± 7%, compared to the lack of insulin stimulation (Fig. 1A, E, and F). Interestingly, PMA did not inhibit p-Tyr of IRS1 in BAEC as previously reported (Fig. 1G) (7).

Identification of serine/threonine phosphorylation sites on IRS2 induced by PMA. The specific sites of p-Ser/Thr on IRS2 induced by PMA in BAEC were identified by tandem mass spectrometry. Analysis of MS2 spectra of tryptic peptides generated from IRS2 revealed serine phosphorylation at three sites (positions 303, 343, and 675) (Fig. 2A). The spectral/peptide match for phosphorylation at Ser303 is shown in Fig. 2B (Mascot score, 45; Sequest Xcorr, 4.48; charge state, 3). Among these residues, three serine residues were selected for further analysis, since they are located in close proximity to functional tyrosine residues (Fig. 2A

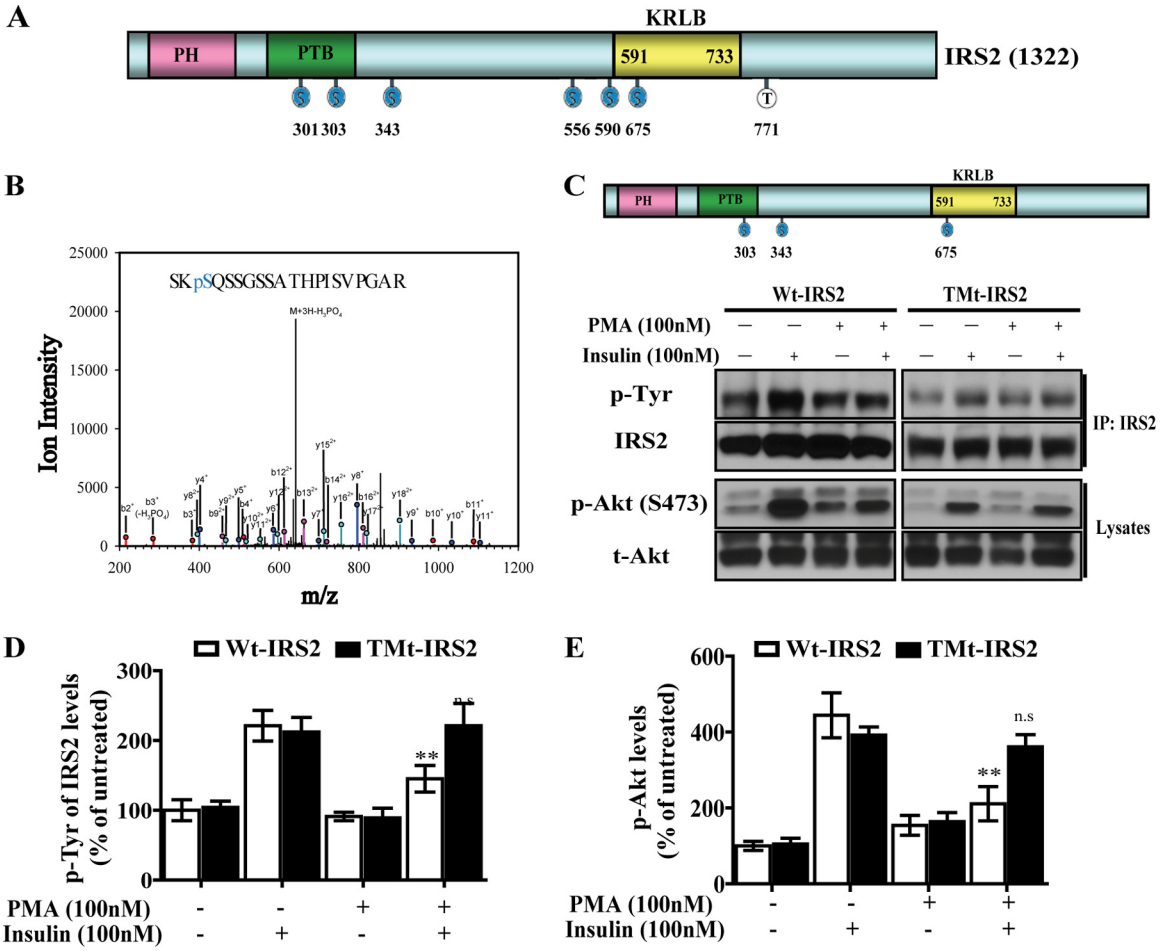

FIG 2 Identification of p-Ser sites on IRS2 induced by PMA. (A) Schematic representation of PMA-induced serine phosphorylation in IRS2. PH, pleckstrin homology domain; PTB, phosphotyrosine-binding domain; KRLB, kinase regulatory-loop binding; S, serine. (B) MS2 spectra corresponding to p-Ser303 of IRS2. (C) Schematic representation of IRS2 mutants used for transfection experiments. The residue numbers correspond to those in the amino acid sequence of mouse IRS2. S303A, S343A, and S675A are the full-length IRS2 mutants that have replacements of the indicated serine residue by alanine. (D) Quantification of p-Tyr levels in IRS2. (E) p-Akt levels in the total cell lysates of BAEC (mean ± SEM, $n = 3$). **, $P < 0.01$, compared to insulin treatment; n.s, not significant.

and B). Ser303 and Ser343 are located in close proximity to phosphotyrosine-binding domain (PTP) and Akt/PKB binding motif, and Ser675 lies within the IRS2-specific KRLB domain and its tyrosine phosphorylation site (p-Tyr671), adjacent to a PI3 kinase binding motif (Fig. 2A). These serine sites on IRS2 (Ser303, Ser343, and Ser675) were mutated by using site-directed mutagenesis, which replaced serine with alanine (TMt-IRS2; S303A, S343A, and S675A). Insulin stimulation of BAEC transiently transfected with wild-type IRS-2 (WT-IRS2) or TMt-IRS2 did not differ (Fig. 2C and D). However, PMA inhibited insulin activation of p-Akt in BAEC expressing WT-IRS2 by 47% ± 13%, a response that was not observed in cells transfected with TMt-IRS2 ($P < 0.01$ compared to insulin treatment) (Fig. 2C and E), indicating that phosphorylation of one or a combination of serines at 303, 343, and 675 of IRS2 induced by PMA were involved in decreasing insulin's activation of p-Tyr of IRS2 and p-Akt.

Characterization of the effect of specific serine phosphorylation induced by PMA on IRS2 p-Tyr of IRS2. Single-serine mutations (S303A, S343A, or S675A) were generated to determine their individual inhibitory effects on p-Tyr-IRS2 in BAEC when PKC was activated by PMA. BAEC were transiently transfected with WT-IRS2 and SMt-IRS2 (S303A), SMt-IRS2 (S343A), and SMt-IRS2 (S675A) mutants, pretreated with PMA, and stimulated with insulin. Insulin increased p-Tyr of IRS2 equally in BAEC transfected with all Mt-IRS2 mutated at only one of the serine sites of IRS2 (Fig. 3A and B). Transfection of these three single serine mutations in IRS2 did not alter insulin activation of p-Akt in BAEC compared to that in cells transfected with WT-IRS2. However, PMA's inhibitory effect on insulin's induction of p-Akt was significantly prevented with the transfection of SMt-IRS2 (S303A) by 91% ± 13% and with that of SMt-IRS2 (S675A) by 87% ± 17%, but PMA did not alter insulin signaling in cells transfected with SMt-343-IRS2 (Fig. 3A and C). These results suggest that phosphorylation of Ser303 and 675 induced by PMA may inhibit insulin-induced p-Tyr of IRS2 and p-Akt. The MS/MS analysis suggested that insulin-induced phosphorylation of tyrosine 653, 671, and 911 (p-Tyr653, p-Tyr671, and p-Tyr911) on IRS2 in mouse liver may be important for insulin activation of the PI3K/Akt pathway. Thus, we examined whether PMA can inhibit these p-Tyr sites on IRS2 in BAEC with and without overexpressing single-serine mutants of IRS2 when activated by insulin. BAEC, treated with insulin or PMA alone or in combination, were

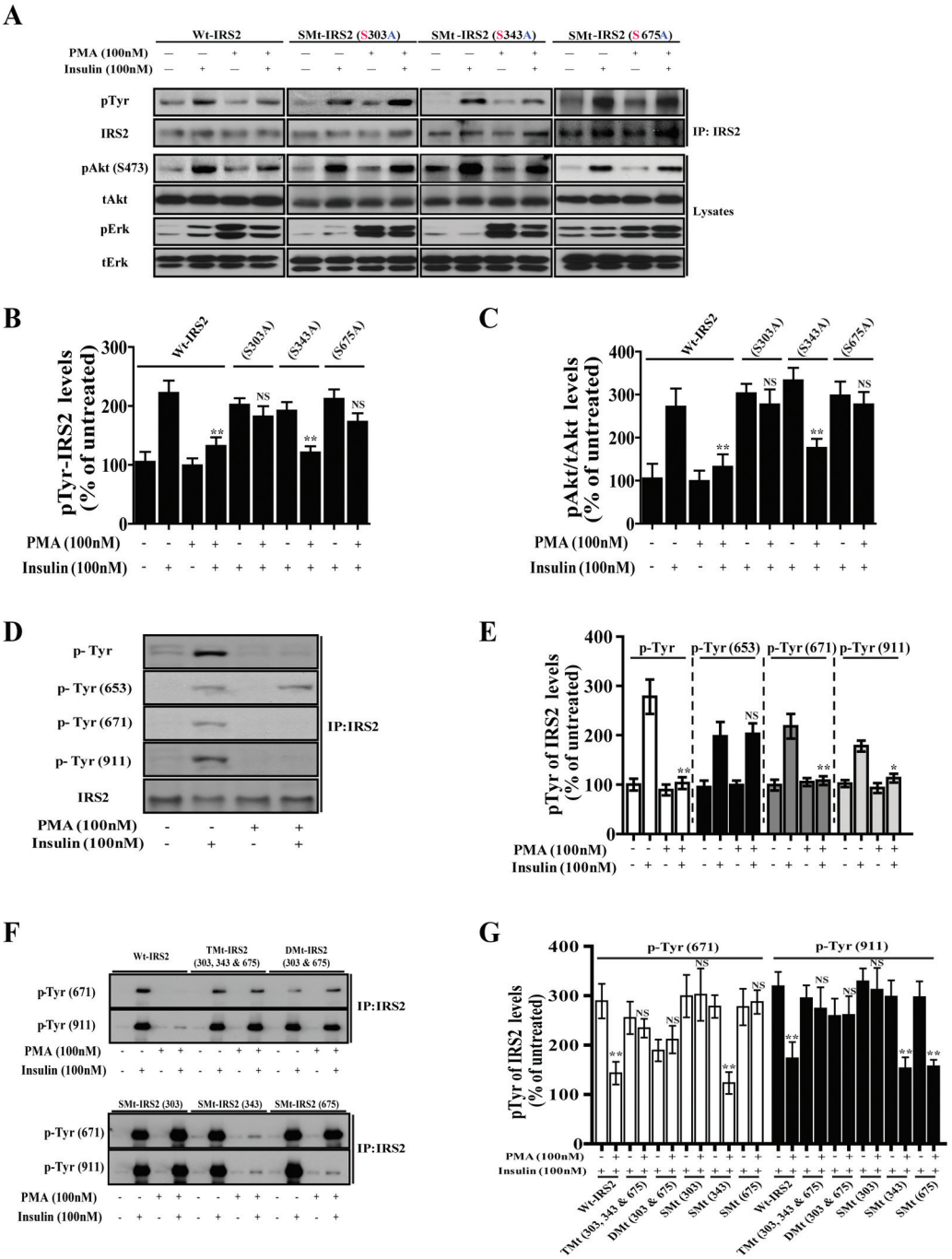

FIG 3 Mutation of serine sites in IRS2 blocks the inhibitory effect of PMA on insulin signaling and selective tyrosine phosphorylation. BAEC were stably transfected with either WT-IRS2 as control or SMt-IRS2 (S303A, S343A, or S675A) and treated with PMA in the absence or presence of insulin. (A) IRS2 was immunoprecipitated with a monoclonal IRS2 antibody, and the blot was probed for p-Tyr (top). Lysates from the same experiment were probed for p-Akt and p-Erk (bottom). (B) Amount of coimmunoprecipitated p-Tyr in IRS-2 was quantified and normalized by IRS2 (mean ± SEM, $n = 4$; **, $P < 0.05$ compared to insulin; NS, not significant). (C) Quantification of p-Akt is shown. (D) Representative immunoblot for three p-Tyr sites (positions 653, 671, and 911) after IP is shown. (E) Quantification of p-Tyr653, p-Tyr671, and p-Tyr911 of IRS2 (mean ± SEM, $n = 5$). (F) Representative immunoblot for p-Tyr671 and p-Tyr911 of IRS2 in BAEC, overexpressing the WT-IRS2, TMt-IRS2 (S303A, S343A, and S675A), DMt-IRS2 (S303A and S675A), or SMt-IRS2 (S303A, S343A, or S675A) under the same conditions as those used for panel A. (G) Quantification of p-Tyr671 and p-Tyr911 of IRS2 (mean ± SEM, $n = 5$; **, $P < 0.05$ compared to insulin; NS, not significant).

immunoprecipitated with polyclonal IRS2 antibody and immunoblotted with phosphor-site-specific antibodies. All three IRS2 tyrosine residues were phosphorylated with the addition of insulin, whereas only p-Tyr671 and p-Tyr911 were inhibited completely by PMA, suggesting that the reduction of tyrosine phosphorylation at positions 671 and 911 on IRS2 impaired insulin signaling (Fig. 3D and E). To identify which serine site of IRS2 affects insulin-stimulated tyrosine phosphorylation at positions 671 and 911, BAEC overexpressing either WT-IRS2 or a serine IRS mutant (TMt-IRS2, DMt-IRS2, or SMt-IRS2) were treated with PMA, followed by stimulation with insulin, and the lysates were immunoprecipitated with anti-IRS2 and immunoblotted for either p-Tyr671 or p-Tyr911 antibodies. The results showed that the mutation of a single serine phosphorylation site (S303A) significantly prevented PMA's inhibition of both p-Tyr sites (671 and 911), whereas mutation of serine 675 (S675A) in IRS2 only decreased PMA's inhibition of insulin-induced p-Tyr671 of IRS2 (Fig. 3F and G).

Activation of PKCβ2 and PKCε induced serine phosphorylation and reduced tyrosine phosphorylation of IRS2. To identify the PKC isoforms activated by PMA responsible for phosphorylating IRS2 on Ser303 and Ser675, adenoviral overexpression of conventional and novel PKC isoforms (α, β1, β2, δ, and ε) was used to test whether p-Tyr of IRS2 is suppressed in insulin-treated BAEC when each PKC isoform is overexpressed. Only the expression of PKCβ2 and PKCε significantly reduced insulin-dependent p-Tyr of IRS2, by 44% ± 15% and 57% ± 19%, respectively (Fig. 4A and B). PKCβ2 was studied further, since it has been shown to be activated by diabetes and AngII in endothelial cells (Fig. 5) (7). To determine whether PKCβ2 can specifically phosphorylate IRS2, we characterized insulin's effect on p-Tyr671 and p-Tyr911 of IRS2 in primary LEC cultured from WT mice or transgenic mice overexpressing PKCβ2 targeted to endothelial cells via the VE-cadherin promoter. Capillary LEC from PKCβ2 transgenic mice exhibited increases in the protein level of PKCβ2 10-fold. These cells lost insulin-induced phosphorylation at p-Tyr671 and p-Tyr911 of IRS2 (Fig. 4C and D). To further confirm the inhibitory effects of PKCβ2 insulin-induced p-Tyr671 and p-Tyr911 of IRS2, the levels of the insulin-mediated p-Tyr671 and p-Tyr911 in BAEC overexpressing either WT-PKCβ2 or dominant negative PKCβ2 (PKCβ2-DN) were studied. The overexpression of Ad-PKCβ2-DN in BAEC inhibited PMA-induced p-Ser303 and p-Ser675 of IRS2 and completely rescued insulin-induced phosphorylation of p-Tyr671 and p-Tyr911 of IRS2. In contrast, the overexpression of WT-IRS2 readily phosphorylated Ser303 and Ser675 on IRS2. Further, p-Ser303 and p-Ser675 of IRS2 were inhibited by the PKCβ2 selective inhibitor ruboxistaurin (RBX), and insulin-induced p-Tyr671 and p-Tyr911 of IRS2 were restored in RBX-treated BAEC (Fig. 4E and F). To further confirm that both p-Ser303 and p-Ser675 of IRS2 have functional consequences, we characterized the levels of p-Tyr671 and p-Tyr911 of IRS2 in BAEC expressing various SMt-IRS2 serine-to-alanine mutants (S303A and S675A). Coexpression of SMt-IRS2 (S303A) with WT-PKCβ2 prevented the inhibition of insulin-induced p-Tyr671 and p-Tyr911. The combined expressions of SMt-IRS2 (S675A) and PKCβ2 blocked a reduction of p-Tyr911, indicating that p-Ser303 has major effects on decreasing insulin-mediated p-Tyr on IRS2 by PKCβ2 (Fig. 4G and H). To determine whether PKCβ2 directly phosphorylates p-Ser 303/675 of IRS2, we performed a co-IP-based *in vitro* PKCβ2 enzymatic assay. The coprecipitation and reverse-precipitation assays showed that PKCβ2 was coimmunoprecipitated in p-Ser303/675, not in p-Ser343, suggesting that PKCβ2 induces p-Ser303/675 of IRS2 (Fig. 6). To determine whether silencing of PKCβ2 expression by small interfering RNA (siRNA) could restore insulin-induced p-Tyr671 and p-Tyr911 of IRS2 in the presence of AngII, we evaluated the effects of PKCβ2 siRNA on p-Tyr671 and p-Tyr911 levels and the level of p-Ser303 of IRS2 in the absence and presence of AngII. As shown by immunoblot analysis, the PKCβ2 siRNA decreased PKCβ2 levels by 83% ± 11% in ZL or ZF-LEC (Fig. 7A), while insulin increased the levels of p-Tyr671 and p-Tyr911 of IRS2 in the ZF-LEC by 198% ± 14% and 205% ± 21%, respectively, with or without AngII (Fig. 7A to C). Furthermore, we observed that the Akt pathway was also significantly enhanced by PKCβ2 siRNA in the absence and presence of AngII (data not shown). PKCβ2 siRNA significantly decreased AngII-mediated p-Ser303 both in the ZL-LEC and in the ZF-LEC (Fig. 7A and D). Taken together, these results suggest that PKCβ2 is most likely the PKC isoform activated by PMA or AngII responsible for phosphorylating Ser303, leading to the inhibition of insulin-induced p-Tyr671 and p-Tyr911 of IRS2 in the endothelial cells.

AngII selectively increased serine phosphorylation of IRS2 through PKCβ2 activation. To evaluate whether physiological activators of PKC can induce phosphorylation on Ser303 and Ser675 of IRS2 to reduce p-Tyr of IRS2, BAEC was stimulated with either AngII, oxidized low-density lipoprotein (Ox-LDL), or tumor necrosis factor alpha (TNF-α) in the presence of insulin, since these proteins have been reported to induce endothelial dysfunction *in vivo* (5, 15, 25). Only stimulation with AngII resulted in decreased p-Tyr of IRS2 in response to insulin (Fig. 8A). To further confirm whether AngII has a similar effect as an activator of PKC, we measured the serine phosphorylation of IRS2 in Ser303 and Ser675. Immunoblot data showed that AngII increased phosphorylation of Ser303, not Ser675, on IRS2 (Fig. 8B and C, bottom). AngII and PMA inhibited total p-Tyr and p-Tyr971 of IRS2, but PMA also inhibited p-Tyr675 (Fig. 8B and C, top). Thus, the findings showed that AngII increased only p-Ser303, not p-Ser675, of IRS2 (Fig. 8D and E). Only serine 303 of IRS2 was phosphorylated by both PMA and AngII, but AngII decreased only insulin-induced p-Tyr911, not p-Tyr671, of IRS2, suggesting that activation of different PKC isoforms by PMA is responsible for the inhibition of insulin-induced p-Tyr671 of IRS2 specifically (Fig. 9). The inhibitory effect of AngII on insulin-stimulated p-Tyr911 on IRS2 was reversed by the antagonist of AngII receptor I losartan (ATR1) (Fig. 8D and E) but not by the ATR2 antagonist (PD12317) of AngII. As shown by immunoblot analysis, AngII increased the activated form of PKCα and PKCβ2 in membrane fractionation 1.4- and 2.2-fold, respectively, but not other PKC isoforms (data not shown). To further document the inhibitory effect of AngII on insulin-induced p-Tyr911, and not p-Tyr671, of IRS2, BAEC were transfected with the SMt-IRS2 (S303A) mutant. Consistent with the result of the losartan treatment, insulin increased tyrosine phosphorylation of IRS2 on Tyr911, and not on Tyr671, in cells expressing the single mutant SMt-IRS2 (S303A) in the presence of AngII (Fig. 8F, bottom), in contrast to WT-IRS2, where p-Tyr911, but not p-Tyr671, of IRS2 was significantly inhibited.

Effect of AngII on insulin-induced tyrosine phosphorylation of IRS2 in PKCβ2-transgenic mice. To further evaluate the inhibitory effect of AngII on insulin-induced p-Tyr911 via PKCβ2

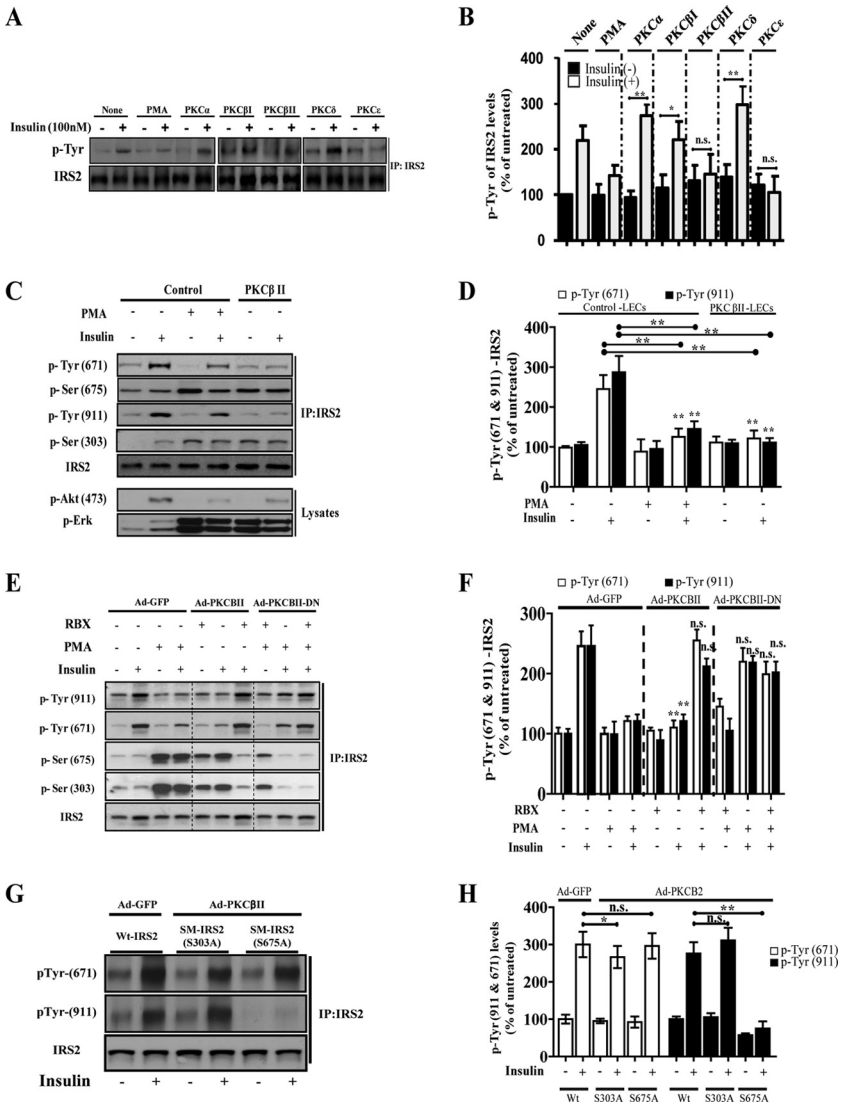

FIG 4 Activated PKCβ2 by PMA induced p-Ser and reduced p-Tyr in IRS2. (A) Immunoblot analysis of tyrosine phosphorylation of IRS2 in lysates from BAEC expressing conventional and novel PKC isoforms in the absence or presence of insulin. (B) p-Tyr of IRS2 level was quantified by densitometry, normalized by IRS2, and expressed as a percentage of the value for untreated BAEC (mean ± SEM, $n = 3$). (C) Immunoblot analysis of phosphorylation of tyrosines (p-Tyr671 or p-Tyr911) or serines (p-Ser303 or p-Ser675) in IRS2 and the insulin signaling pathway in the LEC of PKCβ2 Tg mice or WT mice. (D) Quantification of p-Tyr671, p-Tyr911, p-Ser303, and p-Ser675 levels in IRS2. (E) Immunoblot analysis of p-Tyr or p-Ser in BAEC infected with adenovirus overexpressing PKCβ2, PKCβ2-DN, or GFP as a negative control in the absence or presence of insulin, followed by RBX. (F) Quantification of p-Tyr671 and p-Tyr911 levels in IRS2. (G) Immunoblot analysis for p-Tyr671 and p-Tyr911 of IRS2 in lysates from BAEC expressing SM-IRS2 (S303A) or SM-IRS2 (S675A) in absence or presence of PKCβ2. (H) Quantification of p-Tyr671 and p-Tyr911 levels in IRS2. Data are means ± standard deviations from four determinations. Asterisks indicate statistical significance (**, $P < 0.001$; one-way analysis of variance [ANOVA]).

activation, PKCβ2-Tg and WT mice were infused with AngII or saline, followed by insulin stimulation. As shown by Western blot analysis, insulin increased p-Tyr671 and p-Tyr911 of IRS2 2.7- and 2.9-fold, respectively, compared to the aortas of untreated WT mice. Furthermore, insulin stimulation of PKCβ2-Tg mice increased p-Tyr671 and p-Tyr911 1.6- and 1.8-fold (Fig. 10A to C). AngII infusion further increased levels of p-Ser303 and p-Ser of IRS2 1.5- and 1.3-fold, respectively, in the aortas of PKCβ2-Tg mice, compared to the AngII-injected WT mice (Fig. 10A, D, and E). Furthermore, AngII treatment decreased insulin-induced levels of p-Tyr671 and p-Tyr911 of IRS2 in the aortas of both WT and PKCβ2-Tg mice, compared to those in saline-treated mice (Fig. 10A to C). This result suggests that PKCβ2 activated by AngII inhibits insulin-induced p-Tyr671 and p-Tyr911 of IRS2.

Effect of PMA on insulin-induced association of IR, IRS2, and PI3K. To elucidate the functional effect of Ser303 and Ser675 phosphorylation of IRS2 on insulin activation of protein kinase B (PKB/Akt), we characterized the association of IRS2 and p85α of PI3K in the presence of insulin (7). The association of a series of deletion p85α mutants (Fig. 11A) with IRS2 was analyzed by co-IP experiments in BAEC. As shown in Fig. 11B and C, the addition of insulin increased the association of N- or C-SH2 of p85α (n-SH2 and c-SH2) and IRS2, but no association was noted when insulin was absent. Since the IP experiments showed that IRS2 binding to

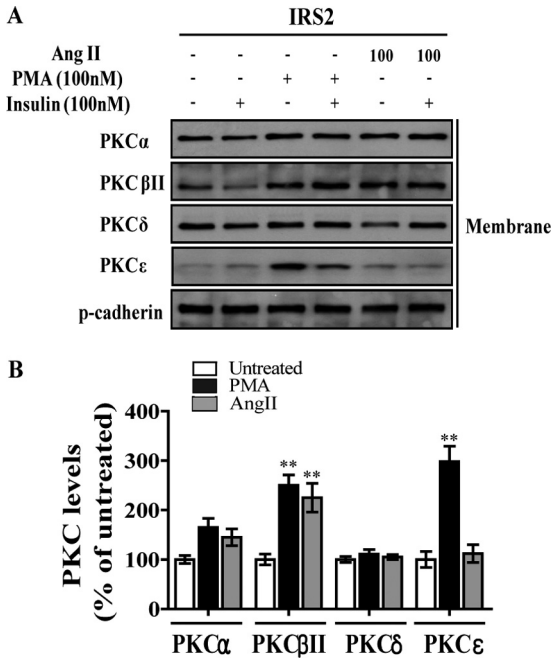

FIG 5 AngII induced and activated PKCβ2 in BAEC with overexpression of IRS2. (A) Immunoblot analysis of activated PKC isoforms in lysates from BAEC expressing conventional and novel PKC isoforms in the absence or presence of AngII. (B) The PKC isoforms levels in membrane of BAEC were quantified by densitometry. Data are means ± standard deviations from four determinations. Asterisks indicate statistical significance (**, $P < 0.001$; one-way ANOVA).

both n-SH2 and c-SH2 of p85α was induced by insulin, we determined whether p-Ser303 and p-Ser675 of IRS2 can influence this association. IRS2 proteins were immunoprecipitated from BAEC overexpressing DMt-IRS2 (S303A and S675A) or WT-IRS2 pretreated with PMA and stimulated with insulin. The results showed that the addition of PMA together with insulin reduced the association of both n-SH2 and c-SH2 of p85α and WT-IRS2 (Fig. 11D, top). However, the inhibition induced by PMA of the binding of IRS2 to p85α in the presence of insulin was prevented in cells overexpressing DMt-IRS2 (Fig. 11D and E, bottom), indicating that p-Ser303 and p-Ser675 of IRS2 induced by PMA are negative regulators of insulin signaling. The reverse coprecipitation using an anti-p85α antibody also confirmed that n-SH2-His and c-SH2-His of p85α were coimmunoprecipitated with IRS2. Further, the IP of p85α, and subsequent detection of p-Tyr-IRS2 by immunoblot analysis, produced only a weak signal (data not shown). In addition, the association of IRS2 with IRβ was also increased by insulin (234% ± 39%) and inhibited by PMA (91% ± 22%) in BAEC overexpressing WT-IRS2. In contrast, association of IRS2 with IRβ in BAEC overexpressing DMt-IRS2 was not inhibited by PMA (Fig. 11F and G).

Serine phosphorylation of IRS2 at positions 303 and 675 *in vivo*. Since all the experiments described above were performed in cultured endothelial cells, we evaluated the effect of insulin on p-Tyr911, p-Ser303, and p-Ser675 of IRS2 in vessels isolated from ZL and ZF rats, which are established models of obesity and insulin resistance (22, 26). Previously, we reported that insulin-stimulated tyrosine phosphorylation of IRS2 proteins and PI3-kinase activation was selectively impaired in vascular tissues from ZF rats compared to ZL rats (26). Thus, ZL and ZF rats were treated with or without insulin intravenously for 10 min, and lysates from the aortic tissues of the ZL and ZF rats were immunoprecipitated with IRS2 antibody, and immunoblotted for p-Ser303 and p-Ser675 (Fig. 12A and B). The results showed that insulin increased p-Tyr911 of IRS2, which was decreased by 46% ± 35% in ZF rats ($P < 0.01$) (Fig. 12A and B). Levels of p-Ser303 and p-Ser675 were significantly, increased in ZF rats compared to ZL rats i.e., by 267% ± 22% and 211% ± 15%, respectively, and these levels were not affected by insulin. Phosphorylation of eNOS, a selective downstream target of IRS2 after activation by insulin in endothelial cells, was also reduced in ZF rats versus ZL rats by 72% ± 31%. To further specifically evaluate the inhibitory effect of AngII on

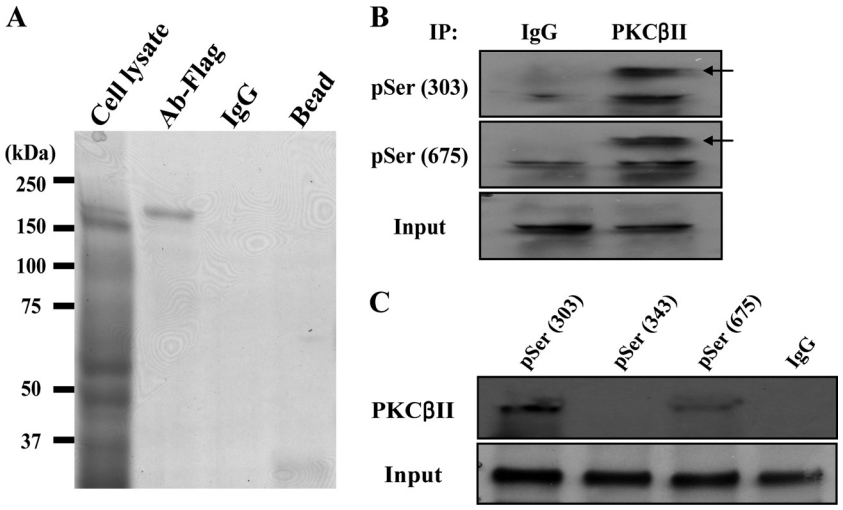

FIG 6 Specific binding of PKCβ2 to the p-Ser303 and p-Ser675 of IRS2. (A) IRS2 was expressed in HEK293 cells and purified with anti-Flag antibody or IgG antibody or with beads as a control. Purified recombinant IRS2 protein was stained with Coomassie dye. (B and C) The purified IRS2 protein was incubated with PKCβ2 enzyme and precipitated with IRS2 antibody or PKCβ2 antibody. (B) The precipitates obtained with PKCβ2 antibody were immunoblotted with antibodies to p-Ser303 or p-Ser675 of IRS2. (C) The precipitates obtained with PKCβ2 antibody were immunoblotted with the specific antibodies for p-Ser303, p-Ser343, or p-Ser675 of IRS2.

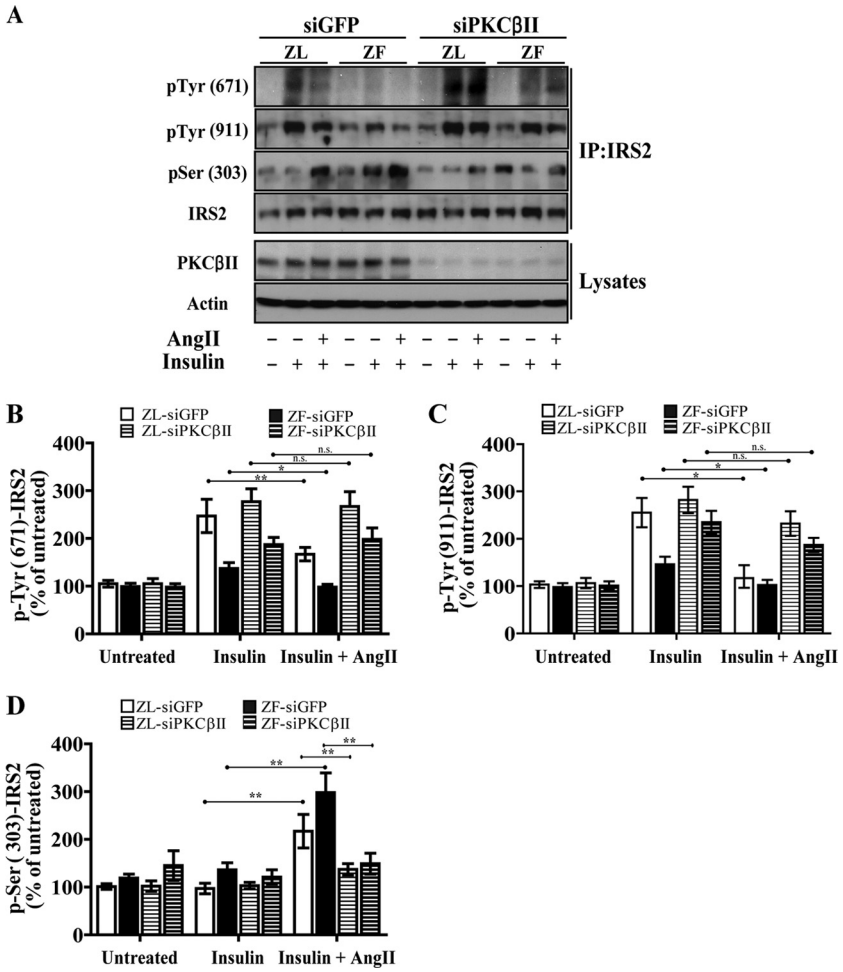

FIG 7 Effect of the PKCβ2 siRNA on tyrosine phosphorylation and serine phosphorylation in ZL-LEC or ZF-LEC. ZL-LEC or ZF-LEC were transfected with either a siRNA specific for PKCβ2 or a control siRNA with a GFP (siGFP). The cells were cultured for 24 h and then treated with insulin in either the absence or presence of AngII. (A) Immunoblot analysis for tyrosine and serine phosphorylation of IRS2 in immunoprecipitates from treated ZL- or ZF-LEC with or without insulin or with insulin plus AngII. (B) The level of p-Tyr671 of IRS2 was quantified by densitometry, normalized to the level of IRS2, and expressed as a percentage of the value for untreated ZL-LEC (mean ± SEM, $n = 3$). (C) Quantification of p-Tyr911 level in IRS2. (D) Quantification of p-Ser303 level in IRS2. Data are means ± standard deviations from four determinations. Asterisks indicate statistical significance (**, $P < 0.001$; one-way ANOVA).

insulin signaling and insulin-induced p-Tyr of IRS2 *in vitro*, we cultured the primary ZL-LEC or ZF-LEC to measure the p-Tyr671, p-Tyr911, and p-Ser303 of IRS2 in LEC treated with AngII alone or in combination with losartan or RBX, in the presence or absence of insulin stimulation. Immunoblot data showed that both losartan and RBX suppressed AngII-induced p-Ser and restored insulin-mediated p-Tyr of IRS2 in ZL-LEC and ZF-LEC (Fig. 12C to E). These results indicate that p-Ser303 and p-Ser675 of IRS2 induced by AngII could block insulin signaling through dephosphorylation of p-Tyr671 and p-Tyr911 in the endothelium of the aorta in the endothelial dysfunctional state *in vivo*.

DISCUSSION

Some of insulin's actions on endothelial cells are vasospecific, such as those mediated via the IRS1/PI3K/Akt pathway. These effects include the activation of eNOS and expression of HO-1 (3). The selective inhibition of insulin signaling via the IRS/PI3K/p-Akt pathway has been demonstrated to induce endothelial dysfunction *in vitro* and *in vivo*, such as in diabetes and insulin-resistant states (4, 27, 28). PKC activation, especially that of the β isoform, has been particularly noted to be associated with these states and to accelerate the development of atherosclerosis and selectively inhibit insulin activation of IRS1/p-Akt (22, 26). The targets of PKC activation, which inhibits insulin's activation of p-Akt and p-eNOS in the endothelial cells, appear to be very different from those in other cells. Recently, a group showed that PKCβ2 expression is increased and inversely correlated with flow-mediated dilation in endothelial cells from patients with type II diabetes (29). They also observed that treatment with LY379196, a PKCβ2 inhibitor, improves insulin-induced p-eNOS in diabetic endothelial cells (29). Multiple sites on IR and IRS1 have been identified as targets of PKC phosphorylation (7, 30, 31). However, unlike findings obtained with other cells, our findings in this study and previous publications have shown that PKC activation by either the chemical activator PMA or the physiological hormone AngII affected only IRS2 and p85/PI3K (7). The mechanisms responsible for the lack of effect of PKC in directly phosphorylating IR and IRS1 in endothelial cells are not clear. It is possible that the differ-

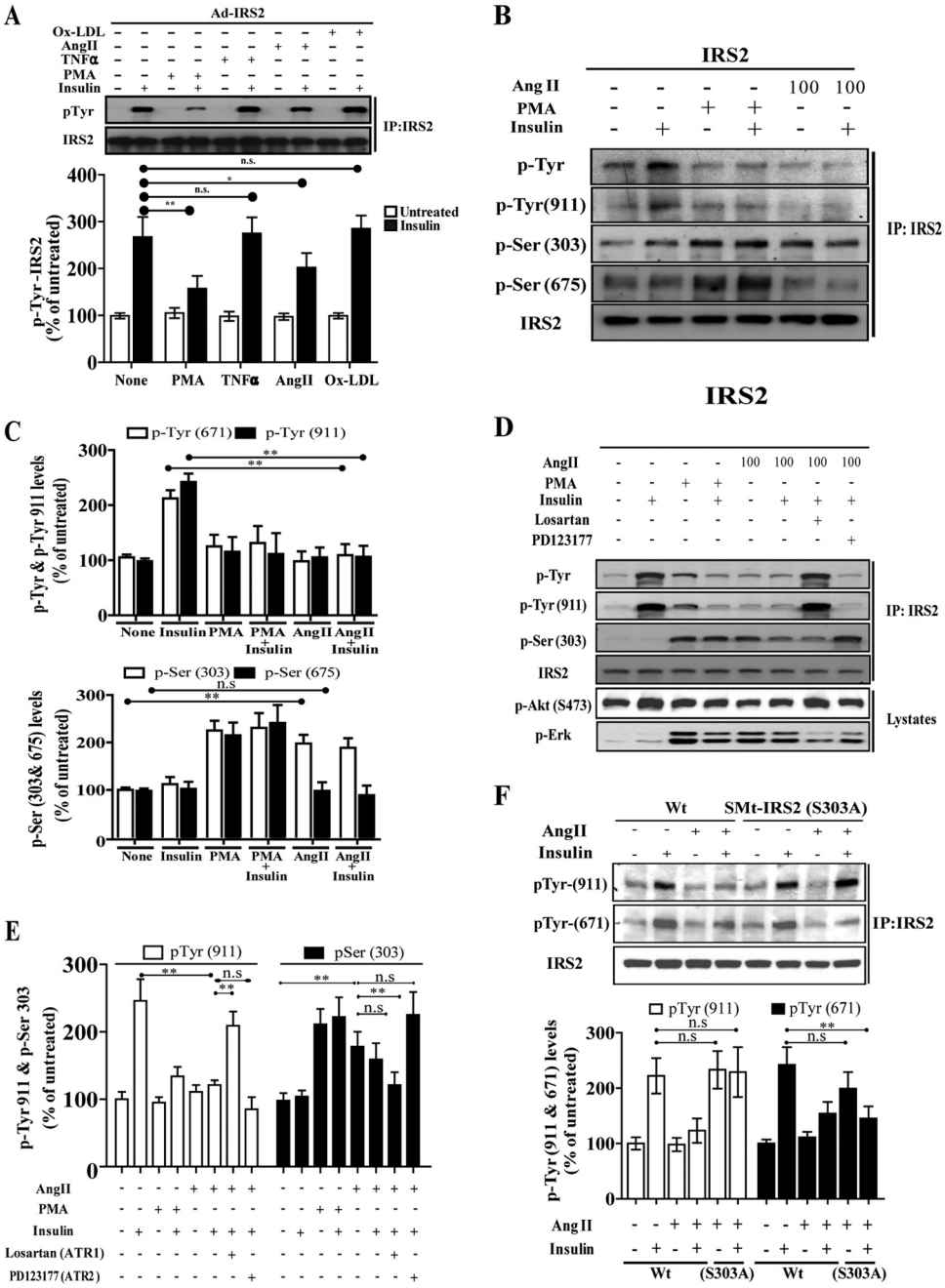

FIG 8 AngII selectively increased serine phosphorylation of IRS2 in a PKCβ2-dependent manner. After being infected with adenoviral constructs expressing WT-IRS2 for 24 h, BAEC were incubated with TNF-α, AngII, or Ox-LDL in the presence or absence of insulin for 10 min. (A) Immunoblot analysis of p-Tyr in immunoprecipitates with anti-IRS2 antibody (top) and quantification of p-Tyr levels in IRS2 (bottom). (B) After the same treatment with AngII as described for panel A, immunoblot analysis of p-Tyr, p-Tyr911, p-Ser303, and p-Ser675 in immunoprecipitates with anti-IRS2 antibody was carried out. (C) Levels of p-Tyr or p-Tyr911 (top) or p-Ser303 and p-Ser675 (bottom) in IRS2 were quantified by densitometry and expressed as a percentage of that in untreated cells (mean ± SEM, $n = 3$). (D) Infected BAEC expressing IRS2 were incubated with AngII for 30 min and then treated in the presence of losartan or PD123177 for 10 min. (E) Levels of p-Ser303 or p-Tyr911 in IRS2 were quantified by densitometry and expressed as a percentage of that in untreated cells (mean ± SEM, $n = 3$). (F) Infected BAEC expressing WT-IRS2 or IRS2 single mutants (S303A or S675D) were treated with AngII for 10 min and then incubated in the presence or absence of insulin. p-Tyr911 and p-Tyr671 were quantified by densitometry, and levels are expressed as percentages of that in untreated cells (mean ± SEM, $n = 3$).

ences in the amount of expression of IRS1 and IRS2 between endothelial cells and nonvascular cells like adipocytes partially provide an explanation (32, 33). In addition, PKC isoform expression and activation induced by various stimuli among the diverse cell types could also be different and contribute to the differences in PKC targets and responses.

Our results indicate the importance of IRS2 in mediating insulin signaling and actions in endothelial cells. Similarly, these findings strongly suggest a role for AngII in causing endothelial dysfunction, since its activation of PKC inhibited over 50% of insulin's activation of p-Akt and p-eNOS, which are mediated partially by decreases in p-Tyr of IRS2. Since AngII activation is

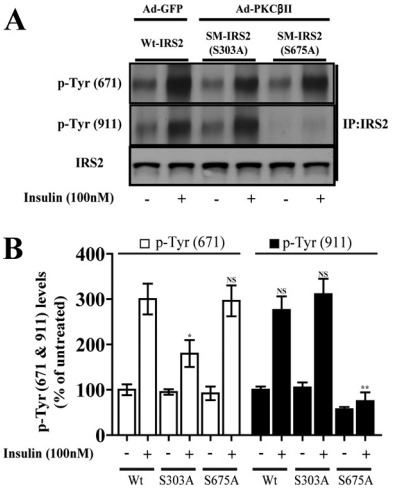

FIG 9 Mutation of serine 303 in IRS2 blocks the inhibitory effect of PKCβ2 on insulin-increased tyrosine phosphorylation at positions 675 and 911. (A) Immunoblot analysis for p-Tyr671 and 911 of IRS2 in lysates from BAEC expressing PKCβ2 by adenoviral infection of PKCβ2 in absence or presence of insulin. (B) The p-Tyr671 and p-Tyr911 levels of IRS2 were quantified by densitometry. Data are means ± standard deviations of four determinations. Asterisks indicate statistical significance (**, $P < 0.001$; one-way ANOVA).

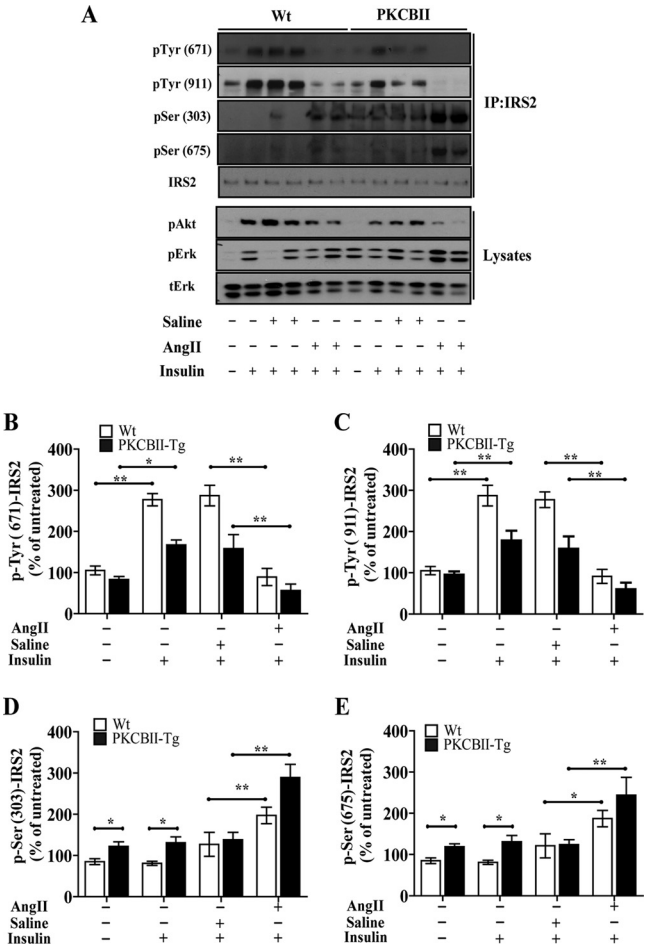

FIG 10 AngII induced serine phosphorylation and tyrosine phosphorylation in IRS2 via PKCβ2 activation. (A) Immunoblot analysis for serine and tyrosine phosphorylation of IRS2 in immunoprecipitates from aortas of infused control or PKCβ2 Tg mice. (B) Quantification of p-Tyr671 level of IRS2. (C) Quantification of p-Tyr911 level of IRS2. (D) Quantification of p-Ser303 level of IRS2. (E) Quantification of p-Ser675 level of IRS2. Data are means ± standard deviations from four determinations. Asterisks indicate statistical significance (**, $P < 0.001$; one-way ANOVA).

associated with acceleration of atherosclerosis in apoE$^{-/-}$ mice, these results also suggest that PKC activation and inhibition of IRS2 could mediate its atherogenic actions. The importance of IRS2 has been suggested by Kubota et al. (34), who reported that endothelial cell-specific IRS2, or IRS1/2 KO, impaired IRS/PI3K/Akt/eNOS activation with systemic insulin resistance, glucose intolerance, and vascular intimal hyperplasia after injury, but its effects on atherosclerosis have not been reported. The regulation of IRS2 by PKC activation has not been reported. In contrast, multiple studies have identified serine phosphorylation sites on IRS1 from many species (human and rodents) which negatively regulate its function, including Ser24, Ser267, Ser270, Ser307, Ser332, Ser357, Ser522, Ser617, Ser632/635, Ser662, and Ser1099/1100. Serine kinases that have been implicated in the phosphorylation of these sites include PKC, p70-GSK/mTOR, JNK, and other mitogen-activated protein kinases (MAPK) (15, 17, 31, 35, 36). Our results in this study show for the first time that the sites where insulin induced p-Tyr in IRS2 were similar to those in hepatocytes, i.e., Tyr653, Tyr671, and Tyr911. Two of these p-Tyr sites, which are located in kinase regulatory-loop binding (KRLB) and YΦXM tyrosine residues, correspond to position 653, which interacted with IR, and position 671, which interacted with p85/PI3K (37, 38). Tyr911 is also included in the YΦXM motif, and it is a crucial site for binding to Grb2 and activates the Erk pathway in 3T3-L1 adipocytes (39). However, in this study, we showed that PMA inhibited insulin-induced p-Tyr911 of IRS2 in endothelial cells, yet MAP kinase activities were elevated. These findings suggest that the mechanism of p-Tyr911 function is insulin dependent in vascular and nonvascular cells. Interestingly, activation of PKC by PMA, which activates both classical and novel PKC isoforms, inhibited only p-Tyr671 and p-Tyr911 induced by insulin. Since both p-Tyr653 and p-Tyr671 are located in the KRLB region of IRS2, it is likely that p-Tyr671 and p-Tyr911 are essential for mediating insulin's vasospecific actions in endothelial cells, since PKC activation completely inhibited insulin's induction of p-Akt or p-eNOS in endothelial cells. Further studies will be needed to identify the roles of p-Tyr653 and p-Tyr911 of IRS2 in insulin's metabolic actions and MAP kinase activation in endothelial cells.

Mass spectrometry analysis documented three sites of phosphorylation on IRS2 that were induced by PKC activation. Site-specific mutagenesis studies indicated that at least two serines, Ser303 and Ser675, of IRS2 are phosphorylated by PKC activation, both of which are involved in PTP or KRLB domain, next to the PI3K binding motif. The importance of these p-Ser sites was clearly shown to be to decrease association of IRS2 with p85α and IR. Since increases of Ser303 and Ser675 on IRS2 decreased its association with both IRβ and p85α/PI3K, it is likely that all insulin actions mediated via IRS2 will be inhibited by PKC activation.

Previously, a few p-Ser sites on IRS2 had been identified. Two serine/threonine sites are described as potential targets of JNK (40, 41). Phosphorylation of Thr348 in IRS2, a functional homolog of Ser307 in IRS1, has been reported to negatively regulate insulin signaling in hepatic cells (41). Another report showed that JNK

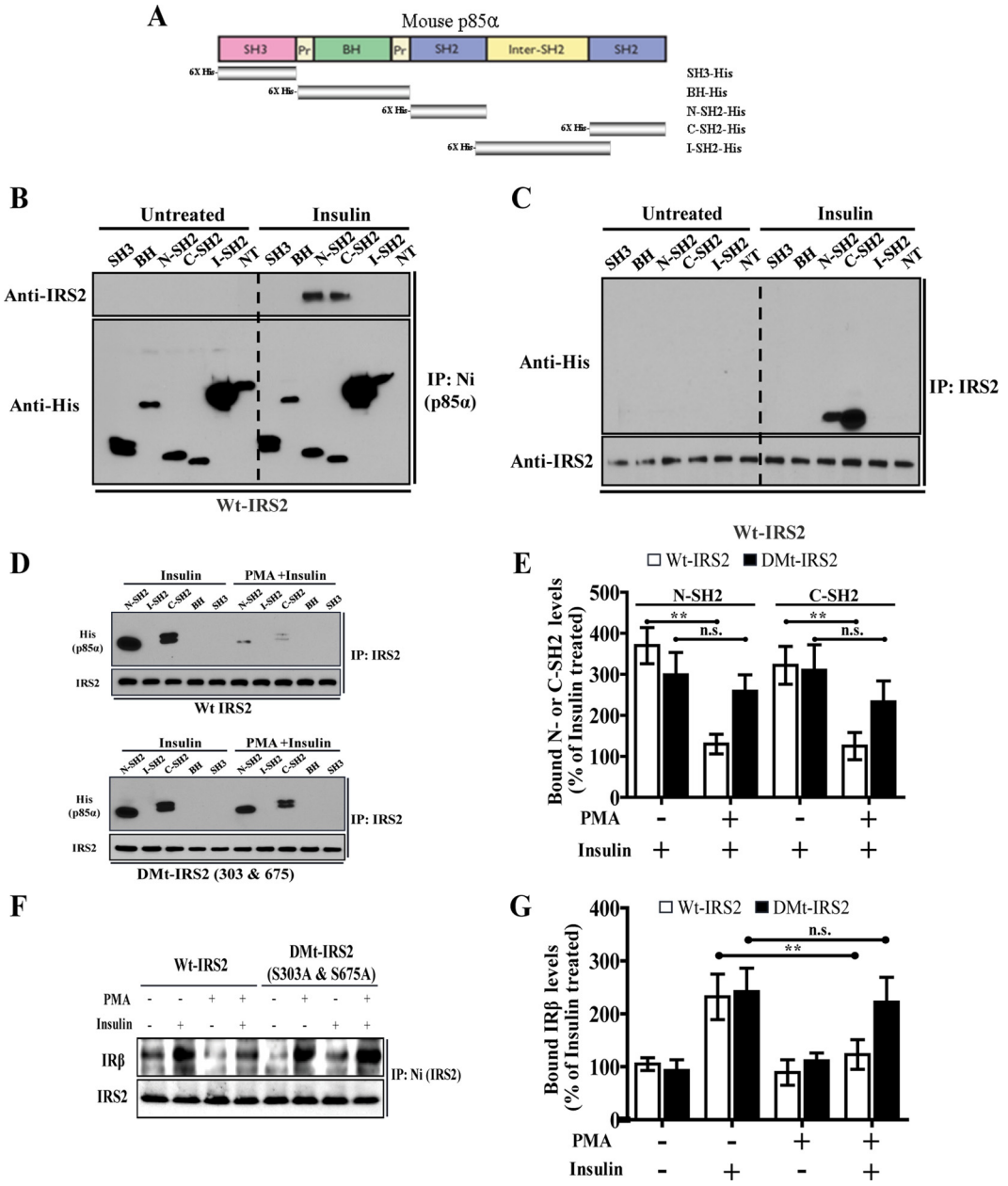

FIG 11 Insulin-induced association of IRS2 and PI3K or IR was interrupted by PMA. (A) Schematic illustration of p85α deletion mutants in PI3K. SH3, Src homology 3 domain; BH, breakpoint cluster region homology domain; C-SH2, C-terminal Src homology 2 domain; N-SH2, N-terminal Src homology 2 domain; I-SH2, internal Src homology 2 domain; NT, N-terminal domain. (B and C) The recombinant SH3-His, BH-His, C-SH2-His, N-SH2-His, I-SH2-His, and NT-His were incubated with lysates from BAEC overexpressing IRS2 in the absence or presence of insulin and precipitated with Ni-resin or an antibody specific for IRS2. The precipitates were immunoblotted with anti-IRS2 (B) or anti-His (C) antibodies. (D and E) The lysates from BAEC expressing WT-IRS (top) or DMt-IRS2 (S303A and S675A) (bottom), treated with PMA in the absence or presence of insulin, were incubated with the p85α deletion mutants and precipitated with anti-IRS2 antibody. The precipitates were immunoblotted with anti-His antibody. (F and G) Blocking of the insulin-induced binding of IRS2 to IR by PMA was inhibited in lysates of BAEC expressing DMt-IRS2.

induces p-Ser of IRS2 on Ser488, which is a prerequisite for the glycogen synthase kinase 3β (GSK-3β)-dependent p-Ser of IRS2 on 484 in hepatocytes (40). However, these p-Ser sites were not detected in endothelial cells. Besides IRS2, PKC activation induced by PMA and AngII can also inhibit insulin-induced phosphorylation of PI3K/eNOS at Thr86, which decreased its association to IRS1/2 (7). Hence, these findings strongly demonstrated that IRS2 is differentially regulated by metabolic factors and plays a dominant functional role in mediating insulin's vasospecific effects on endothelial cells.

Our study focused on the PKC-specific sites, since multiple reports have shown that several PKC isoforms are activated by diabetes and its associated metabolites, such as elevated levels of glucose and free fatty acids (20, 25, 42). PMA can activate both classical and novel PKC isoforms in endothelial and other cells. However, physiological activation of PKC and PKCα and -β iso-

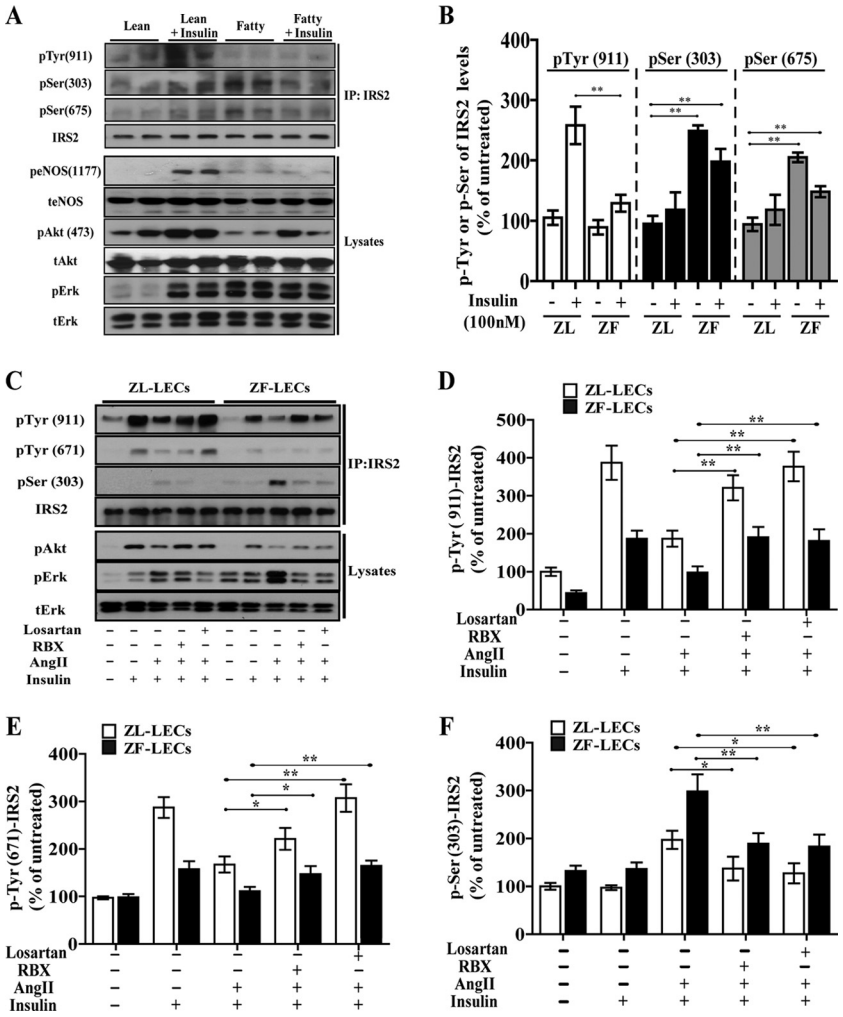

FIG 12 Serine and tyrosine phosphorylation of IRS2 *in vivo*. (A) Lysates of the aortas of 12-week-old ZL or ZF rats 5 min after intraperitoneal injection of insulin or vehicle as described in Materials and Methods were subjected to IP using anti-IRS2. The precipitated proteins were analyzed by immunoblotting using anti-p-Tyr, p-Ser, or anti-IRS2 (top). Immunoblot analysis of insulin signaling pathway in lysates from aortas of ZL or ZF rats (bottom). (B) The p-Tyr and p-Ser levels of IRS2 were quantified by densitometry. Data are means ± standard deviations from four determinations. (C) Immunoblot analysis for p-Tyr671, p-Tyr911, and p-Ser303 of IRS2 in lysates from ZL- or ZF-LEC incubated without or with insulin in the absence or presence of AngII plus losartan or RBX. (D and E) Quantification of p-Tyr671 (D) and p-Tyr911 (E) levels in IRS2. (F) Quantification of p-Ser303 levels in IRS2. Asterisks indicate statistical significance (*, $P < 0.05$; **, $P < 0.001$; one-way ANOVA).

forms by AngII induced only p-Ser303 and inhibited only p-Tyr911 of IRS2 induced by insulin (Fig. 5). The physiological importance of these changes in p-Tyr911 and p-Ser303/Ser675 is supported by the *in vivo* results using aortas from ZL or ZF rats, an established rodent model of insulin resistance and obesity, which we and others have previously reported to manifest endothelial dysfunction, and selective inhibition of insulin's activation of PI3K/Akt/eNOS cascade due to PKCβ activation (Fig. 12) (26). Furthermore, AngII further increased p-Ser303 and p-Ser675 and inhibited insulin-induced p-Tyr671 and p-Tyr911 of IRS2, as shown by the immunoblot assay in aortas of PKCβ-Tg mice (Fig. 10). Silencing PKCβ2 expression by siRNA attenuated the inhibitory effect of AngII on activation of the insulin signaling pathway, further supporting the role of AngII via PKCβ2 as an endogenous inhibitor of the insulin signaling pathway (Fig. 7). These findings have identified for the first time a p-Tyr911 of IRS2, which is inhibited by PKCβ activation via increasing p-Ser303. Interestingly, both p-Ser303 and p-Ser675 were increased in the aortas of ZF rats and AngII-treated PKCβ2-Tg mice, whereas PKCα and -β increased only p-Ser303/IRS2. This indicates that other cytokines or metabolites that are elevated in ZF rats and AngII-treated PKCβ2-Tg mice may activate other PKC isoforms, such as PKCδ and -ε, to induce p-Ser675 of IRS2 and possibly inhibit p-Tyr671 (Fig. 13). Further physiological studies will be needed to elucidate the selective functions of p-Tyr671 of IRS2 in endothelial cells.

In conclusion, the present study provides the first biochemical understanding of the interactions of p-Ser/Thr sites with p-Tyr sites on IRS2, which can affect insulin-induced vasospecific actions in endothelial cells. These findings have identified two novel p-Ser sites on IRS2 by which AngII, via PKC activation, can inhibit insulin-induced p-Tyr and insulin signaling through the IRS2/PI3K/Akt pathway in endothelial cells. We also showed that PKCβ2 can induce p-Ser 303/675 of IRS2 directly by coincubating *in vitro* PKCβ2 with purified IRS2 and demonstrated that the ser-

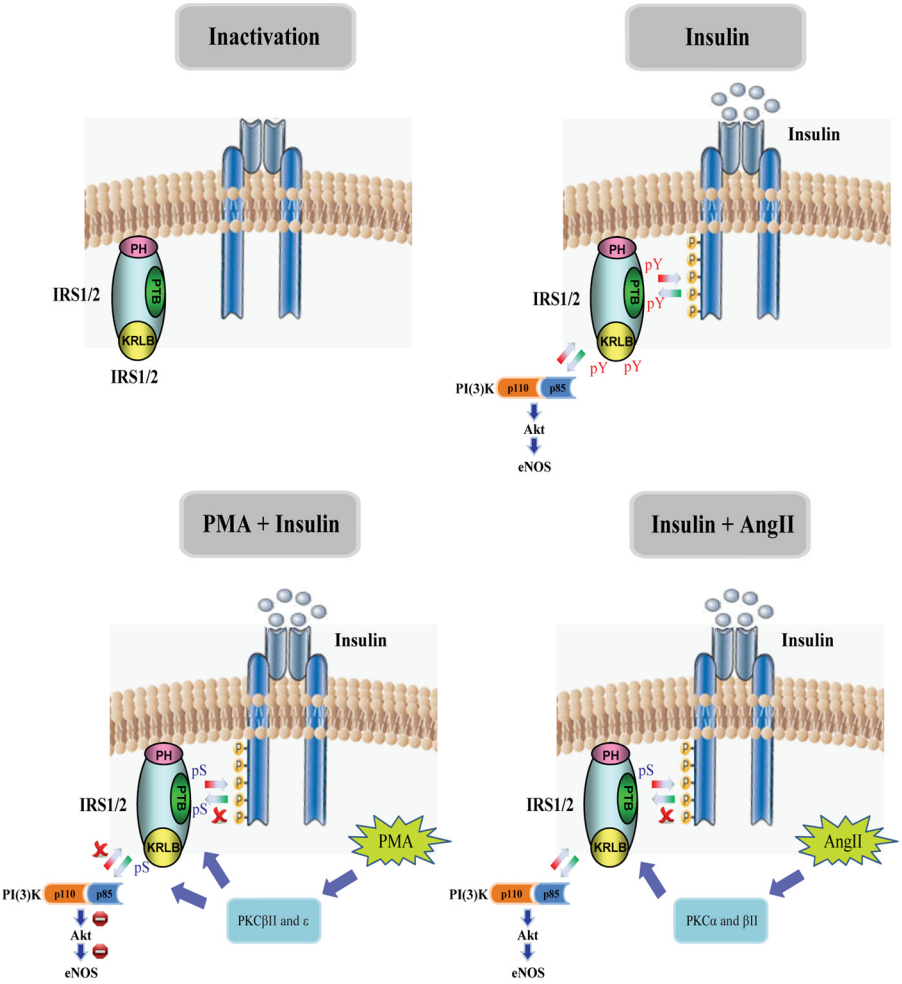

FIG 13 Model of the inhibitory effect of PMA and AngII on IRS2-dependent insulin signaling. In the presence of PMA, activation of PKCβ2/ε induces p-Ser303 and p-Ser675 and reduces insulin-mediated p-Tyr671 and p-Tyr911 in IRS2. AngII stimulation phosphorylates serine of IRS2 at position 303 and inhibits insulin signaling through disruption of an IR/IRS2 or IRS2/p85 of the PI3K complex on endothelial cells.

ine sites on IRS2 (303/675) were phosphorylated by PKCβ2 (Fig. 6). The identification of p-Ser303 and -675 of IRS2 by AngII, via PKC activation, suggests that these residues could be therapeutic targets for inhibition to improve insulin signaling in the endothelium, which could lead to improvement of endothelial dysfunction commonly observed in insulin-resistant states and diabetes, leading to acceleration of atherosclerosis.

ACKNOWLEDGMENT

This work was supported by the National Institute of Diabetes and Digestive and Kidney Disease (R01DK053105).

REFERENCES

1. **Despres JP, Lamarche B, Mauriege P, Cantin B, Dagenais GR, Moorjani S, Lupien PJ.** 1996. Hyperinsulinemia as an independent risk factor for ischemic heart disease. N. Engl. J. Med. **334:**952–957.
2. **Howard G, O'Leary DH, Zaccaro D, Haffner S, Rewers M, Hamman R, Selby JV, Saad MF, Savage P, Bergman R.** 1996. Insulin sensitivity and atherosclerosis. The Insulin Resistance Atherosclerosis Study (IRAS) Investigators. Circulation **93:**1809–1817.
3. **Geraldes P, Yagi K, Ohshiro Y, He Z, Maeno Y, Yamamoto-Hiraoka J, Rask-Madsen C, Chung SW, Perrella MA, King GL.** 2008. Selective regulation of heme oxygenase-1 expression and function by insulin through IRS1/phosphoinositide 3-kinase/Akt-2 pathway. J. Biol. Chem. **283:**34327–34336.
4. **Rask-Madsen C, Li Q, Freund B, Feather D, Abramov R, Wu IH, Chen K, Yamamoto-Hiraoka J, Goldenbogen J, Sotiropoulos KB, Clermont A, Geraldes P, Dall'Osso C, Wagers AJ, Huang PL, Rekhter M, Scalia R, Kahn CR, King GL.** 2010. Loss of insulin signaling in vascular endothelial cells accelerates atherosclerosis in apolipoprotein E null mice. Cell Metab. **11:**379–389.
5. **Boden G.** 1997. Role of fatty acids in the pathogenesis of insulin resistance and NIDDM. Diabetes **46:**3–10.
6. **Feener EP, King GL.** 1997. Vascular dysfunction in diabetes mellitus. Lancet **350**(Suppl. 1):SI9–SI13.
7. **Maeno Y, Li Q, Park K, Rask-Madsen C, Gao B, Matsumoto M, Liu Y, Wu IH, White MF, Feener EP, King GL.** 2012. Inhibition of insulin signaling in endothelial cells by protein kinase C-induced phosphorylation of p85 subunit of phosphatidylinositol 3-kinase (PI3K). J. Biol. Chem. **287:**4518–4530.
8. **Venieratos PD, Drossopoulou GI, Kapodistria KD, Tsilibary EC, Kitsiou PV.** 2010. High glucose induces suppression of insulin signalling and apoptosis via upregulation of endogenous IL-1beta and suppressor of cytokine signalling-1 in mouse pancreatic beta cells. Cell Signal **22:**791–800.
9. **Lee AV, Gooch JL, Oesterreich S, Guler RL, Yee D.** 2000. Insulin-like growth factor I-induced degradation of insulin receptor substrate 1 is mediated by the 26S proteasome and blocked by phosphatidylinositol 3′-kinase inhibition. Mol. Cell. Biol. **20:**1489–1496.

10. **Rui L, Yuan M, Frantz D, Shoelson S, White MF.** 2002. SOCS-1 and SOCS-3 block insulin signaling by ubiquitin-mediated degradation of IRS1 and IRS2. J. Biol. Chem. **277:**42394–42398.
11. **Boura-Halfon S, Zick Y.** 2009. Phosphorylation of IRS proteins, insulin action, and insulin resistance. Am. J. Physiol. Endocrinol. Metab. **296:** E581–E591.
12. **Hanke S, Mann M.** 2009. The phosphotyrosine interactome of the insulin receptor family and its substrates IRS-1 and IRS-2. Mol. Cell. Proteomics **8:**519–534.
13. **Greene MW, Garofalo RS.** 2002. Positive and negative regulatory role of insulin receptor substrate 1 and 2 (IRS-1 and IRS-2) serine/threonine phosphorylation. Biochemistry **41:**7082–7091.
14. **Mothe I, Van Obberghen E.** 1996. Phosphorylation of insulin receptor substrate-1 on multiple serine residues, 612, 632, 662, and 731, modulates insulin action. J. Biol. Chem. **271:**11222–11227.
15. **Aguirre V, Uchida T, Yenush L, Davis R, White MF.** 2000. The c-Jun NH(2)-terminal kinase promotes insulin resistance during association with insulin receptor substrate-1 and phosphorylation of Ser(307). J. Biol. Chem. **275:**9047–9054.
16. **Rui L, Aguirre V, Kim JK, Shulman GI, Lee A, Corbould A, Dunaif A, White MF.** 2001. Insulin/IGF-1 and TNF-alpha stimulate phosphorylation of IRS-1 at inhibitory Ser307 via distinct pathways. J. Clin. Invest. **107:**181–189.
17. **Waraich RS, Weigert C, Kalbacher H, Hennige AM, Lutz SZ, Haring HU, Schleicher ED, Voelter W, Lehmann R.** 2008. Phosphorylation of Ser357 of rat insulin receptor substrate-1 mediates adverse effects of protein kinase C-delta on insulin action in skeletal muscle cells. J. Biol. Chem. **283:**11226–11233.
18. **Zhang J, Gao Z, Yin J, Quon MJ, Ye J.** 2008. S6K directly phosphorylates IRS-1 on Ser-270 to promote insulin resistance in response to TNF-(alpha) signaling through IKK2. J. Biol. Chem. **283:**35375–35382.
19. **Blom N, Gammeltoft S, Brunak S.** 1999. Sequence and structure-based prediction of eukaryotic protein phosphorylation sites. J. Mol. Biol. **294:** 1351–1362.
20. **Das Evcimen N, King GL.** 2007. The role of protein kinase C activation and the vascular complications of diabetes. Pharmacol. Res. **55:**498–510.
21. **Mima A, Hiraoka-Yamomoto J, Li Q, Kitada M, Li C, Geraldes P, Matsumoto M, Mizutani K, Park K, Cahill C, Nishikawa S, Rask-Madsen C, King GL.** 2012. Protective effects of GLP-1 on glomerular endothelium and its inhibition by PKCbeta activation in diabetes. Diabetes **61:**2967–2979.
22. **Naruse K, Rask-Madsen C, Takahara N, Ha SW, Suzuma K, Way KJ, Jacobs JR, Clermont AC, Ueki K, Ohshiro Y, Zhang J, Goldfine AB, King GL.** 2006. Activation of vascular protein kinase C-beta inhibits Akt-dependent endothelial nitric oxide synthase function in obesity-associated insulin resistance. Diabetes **55:**691–698.
23. **Taguchi K, Kobayashi T, Matsumoto T, K Kamata.** 2011. Dysfunction of endothelium-dependent relaxation to insulin via PKC-mediated GRK2/Akt activation in aortas of ob/ob mice. Am. J. Physiol. Heart Circ. Physiol. **301:**H571–H583.
24. **Harja E, Chang JS, Lu Y, Leitges M, Zou YS, Schmidt AM, Yan SF.** 2009. Mice deficient in PKCbeta and apolipoprotein E display decreased atherosclerosis. FASEB J. **23:**1081–1091.
25. **Feener EP, King GL.** 2001. Endothelial dysfunction in diabetes mellitus: role in cardiovascular disease. Heart Fail Monit. **1:**74–82.
26. **Jiang ZY, Lin YW, Clemont A, Feener EP, Hein KD, Igarashi M, Yamauchi T, White MF, King GL.** 1999. Characterization of selective resistance to insulin signaling in the vasculature of obese Zucker (fa/fa) rats. J. Clin. Invest. **104:**447–457.
27. **Mima A, Ohshiro Y, Kitada M, Matsumoto M, Geraldes P, Li C, Li Q, White GS, Cahill C, Rask-Madsen C, King GL.** 2011. Glomerular-specific protein kinase C-beta-induced insulin receptor substrate-1 dysfunction and insulin resistance in rat models of diabetes and obesity. Kidney Int. **79:**883–896.
28. **Symons JD, McMillin SL, Riehle C, Tanner J, Palionyte M, Hillas E, Jones D, Cooksey RC, Birnbaum MJ, McClain DA, Zhang QJ, Gale D, Wilson LJ, Abel ED.** 2009. Contribution of insulin and Akt1 signaling to endothelial nitric oxide synthase in the regulation of endothelial function and blood pressure. Circ. Res. **104:**1085–1094.
29. **Tabit CE, Shenouda SM, Holbrook M, Fetterman JL, Kiani S, Frame AA, Kluge MA, Held A, Dohadwala MM, Gokce N, Farb MG, Rosenzweig J, Ruderman N, Vita JA, Hamburg NM.** 2013. Protein kinase C-beta contributes to impaired endothelial insulin signaling in humans with diabetes mellitus. Circulation **127:**86–95.
30. **Aguirre V, Werner ED, Giraud J, Lee YH, Shoelson SE, White MF.** 2002. Phosphorylation of Ser307 in insulin receptor substrate-1 blocks interactions with the insulin receptor and inhibits insulin action. J. Biol. Chem. **277:**1531–1537.
31. **Liu YF, Herschkovitz A, Boura-Halfon S, Ronen D, Paz K, Leroith D, Zick Y.** 2004. Serine phosphorylation proximal to its phosphotyrosine binding domain inhibits insulin receptor substrate 1 function and promotes insulin resistance. Mol. Cell. Biol. **24:**9668–9681.
32. **Tseng YH, Kriauciunas KM, Kokkotou E, Kahn CR.** 2004. Differential roles of insulin receptor substrates in brown adipocyte differentiation. Mol. Cell. Biol. **24:**1918–1929.
33. **Tseng YH, Ueki K, Kriauciunas KM, Kahn CR.** 2002. Differential roles of insulin receptor substrates in the anti-apoptotic function of insulin-like growth factor-1 and insulin. J. Biol. Chem. **277:**31601–31611.
34. **Kubota T, Kubota N, Kumagai H, Yamaguchi S, Kozono H, Takahashi T, Inoue M, Itoh S, Takamoto I, Sasako T, Kumagai K, Kawai T, Hashimoto S, Kobayashi T, Sato M, Tokuyama K, Nishimura S, Tsunoda M, Ide T, Murakami K, Yamazaki T, Ezaki O, Kawamura K, Masuda H, Moroi M, Sugi K, Oike Y, Shimokawa H, Yanagihara N, Tsutsui M, Terauchi Y, Tobe K, Nagai R, Kamata K, Inoue K, Kodama T, Ueki K, Kadowaki T.** 2011. Impaired insulin signaling in endothelial cells reduces insulin-induced glucose uptake by skeletal muscle. Cell Metab. **13:**294–307.
35. **Gual P, Gremeaux T, Gonzalez T, Le Marchand-Brustel Y, Tanti JF.** 2003. MAP kinases and mTOR mediate insulin-induced phosphorylation of insulin receptor substrate-1 on serine residues 307, 612 and 632. Diabetologia **46:**1532–1542.
36. **Liberman Z, Eldar-Finkelman H.** 2005. Serine 332 phosphorylation of insulin receptor substrate-1 by glycogen synthase kinase-3 attenuates insulin signaling. J. Biol. Chem. **280:**4422–4428.
37. **He W, Craparo A, Zhu Y, O'Neill TJ, Wang LM, Pierce JH, Gustafson TA.** 1996. Interaction of insulin receptor substrate-2 (IRS-2) with the insulin and insulin-like growth factor I receptors. Evidence for two distinct phosphotyrosine-dependent interaction domains within IRS-2. J. Biol. Chem. **271:**11641–11645.
38. **Park SY, Shoelson SE.** 2008. When a domain is not a domain. Nat. Struct. Mol. Biol. **15:**224–226.
39. **Wu J, Tseng YD, Xu CF, Neubert TA, White MF, Hubbard SR.** 2008. Structural and biochemical characterization of the KRLB region in insulin receptor substrate-2. Nat. Struct. Mol. Biol. **15:**251–258.
40. **Sharfi H, Eldar-Finkelman H.** 2008. Sequential phosphorylation of insulin receptor substrate-2 by glycogen synthase kinase-3 and c-Jun NH2-terminal kinase plays a role in hepatic insulin signaling. Am. J. Physiol. Endocrinol. Metab. **294:**E307–E315.
41. **Solinas G, Naugler W, Galimi F, Lee MS, Karin M.** 2006. Saturated fatty acids inhibit induction of insulin gene transcription by JNK-mediated phosphorylation of insulin-receptor substrates. Proc. Natl. Acad. Sci. U. S. A. **103:**16454–16459.
42. **Igarashi M, Wakasaki H, Takahara N, Ishii H, Jiang ZY, Yamauchi T, Kuboki K, Meier M, Rhodes CJ, King GL.** 1999. Glucose or diabetes activates p38 mitogen-activated protein kinase via different pathways. J. Clin. Invest. **103:**185–195.